Spectral-domain phase microscopy

Michael A. Choma, Audrey K. Ellerbee, and Changhuei Yang*

Department of Biomedical Engineering, Duke University, Durham, North Carolina 27708

Tony L. Creazzo

Pediatrics/Neonatology Division, Neonatal/Perinatal Research Institute, Duke University, Durham, North Carolina 27708

Joseph A. Izatt

Department of Biomedical Engineering, Duke University, Durham, North Carolina 27708

Received October 8, 2004

Broadband interferometry is an attractive technique for the detection of cellular motions because it provides depth-resolved phase information via coherence gating. We present a phase-sensitive technique called spectral-domain phase microscopy (SDPM). SDPM is a functional extension of spectral-domain optical coherence tomography that allows for the detection of nanometer-scale motions in living cells. The sensitivity of the technique is demonstrated, and its calibration is verified. A shot-noise limit to the displacement sensitivity of this technique is derived. Measurement of cellular dynamics was performed on spontaneously beating cardiomyocytes isolated from chick embryos. © 2005 Optical Society of America

OCIS codes: 110.4500, 120.3180, 110.0180, 180.3170, 110.4280.

Retrieval of phase information in interferometric-based optical imaging allows for the calculation of subwavelength variations in the position of a reflector. Over the past decade, several phase-sensitive techniques have been developed to study the motion of individual biological molecules[1] and single-cell dynamics.[2,3] Although earlier techniques were unable to obtain depth-dependent phase information,[1,2] Yang *et al.*[3] used the coherence gating properties inherent in optical coherence tomography (OCT) to record phase data from an individual cell and reject phase information from other structures.

A typical OCT system employs a Michelson interferometer illuminated with a broadband light source. This interference signal is recorded either as a function of reference reflector position (time-domain OCT) or as a function of optical wavelength (spectral-domain OCT). The moving reference arm in time-domain OCT typically introduces a significant level of phase noise, and Yang *et al.* compensated for this by measuring interferometer jitter with a cw reference beam that was harmonically related to the OCT center wavelength. Spectral-domain OCT,[4,5] which includes swept source (SS) and Fourier-domain (FD) OCT, offers several advantages over time-domain OCT. First, spectral-domain OCT interferometers do not contain moving parts that can substantially increase the phase noise floor. Moreover, because spectral-domain OCT interferometers do not require a scanning delay line, they can be built using a common-path topology[4] in which virtually all phase noise is common mode between the reference and sample optical fields.

Here we describe spectral-domain phase microscopy (SDPM), a phase-sensitive functional derivative of spectral-domain OCT that allows for real-time measurement of displacements with picometer-to-nanometer-scale sensitivity. We demonstrate SDPM using both FD and SS interferometers and show the measurement of isolated myocyte contractions with a FD SDPM system mounted on a standard inverted microscope.

Consider the common-path FD and SS OCT interferometers in Fig. 1. The interferometric signal spans an optical bandwidth $\Delta k = k_{\max} - k_{\min}$. The reflection from the bottom surface of a coverslip serves as the reference electric field,[4] while the reflections from cells resting on the top surface constitute the sample field. The detector signal contains an interferometric component that contains information about the amplitude and the phase of the sample optical field. In the case of a single sample reflector this interferometric component is given by

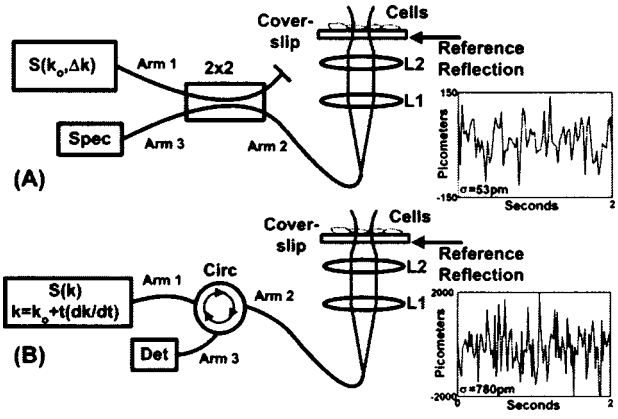

Fig. 1. (a) FD SDPM interferometer. The source is a ~5 mW with a center wavelength and a 3-dB bandwidth of 830 and 45 nm, respectively. The spectrometer (Spec) has a 25-ms readout rate and a 5-ms integration time. (b) SS SDPM interferometer. The narrow-linewidth source is swept through a 130-nm bandwidth over 5 ms with a center wavelength of 1310 nm and an average power of ~3 mW (Micron Optics[5]). The insets show the displacement signals recorded from a clean coverslip.

0146-9592/05/101162-3/$15.00

$$\tilde{i}(k) = (\rho/e)S(k)\delta k \Delta t \sqrt{R_R R_S}\cos[2nk(\Delta x + \delta x)]. \quad (1)$$

Here $\Delta x + \delta x$ is the free-space distance between the reference and sample reflectors, and n is the average group index between the reference and sample reflectors. Δx denotes the position of the sample reflector as in conventional OCT, i.e., to within the full width at half-maximum axial resolution given by the source coherence length, while δx accounts for subresolution or subcoherence length deviations of the reflector from Δx. $S(k)$ is the source power density function; δk is the spectrometer spectral resolution; Δt is the time to acquire a one-dimensional reflectivity profile or A-scan; R_R and R_S are the reference and sample reflectivities, respectively; ρ is the detector responsivity; and e is the electronic charge.

Fourier transformation of $\tilde{i}(k)$ yields an A-scan $\tilde{I}(x)$ that has peak values at $x = \pm 2n\Delta x$. $\tilde{I}(x)$ evaluated at $x = \pm 2n\Delta x$ is

$$\tilde{I}(\pm 2n\Delta x) = (\rho/2e)S\Delta t\sqrt{R_R R_S}E(2n\Delta x)\exp(\pm j2k_0 n\delta x), \quad (2)$$

where S is the total source power, $E(2n\Delta x)$ is the unity-amplitude coherence envelope function, and k_0 is the source center wave number. Since the phase of $\tilde{I}(\pm 2n\Delta x)$ is a linear function of δx, time-varying changes in the subresolution position of the sample reflector can be measured with respect to an arbitrary zero point taken at a reference time t_0:

$$\delta x(t) = \lambda_0/4n\pi[\angle\tilde{I}(2n\Delta x, t) - \angle\tilde{I}(2n\Delta x, t_0)], \quad (3)$$

where $\angle$ is the phase operator and λ_0 is the source center wavelength.

Equations (2) and (3) demonstrate that subresolution changes in reflector position can be tracked over the region where the coherence envelope sits over the noise floor, provided that δx varies slowly enough with respect to the system line rate to allow for phase unwrapping. Equation (3) makes the assumption that changes in optical path length (OPL) are dominated by changes in absolute path length and that changes in optical index are negligible. It likewise should be noted that SDPM can be used to track small changes in the optical index of a sample, provided that changes in absolute path length are negligible.

A fundamental lower limit on the displacement sensitivity of $\delta x(t)$ as a result of shot noise may be derived by generalizing $\tilde{i}(k)$ to contain an additive, uncorrelated Gaussian white-noise term $a(k)$. The A-scan is given by the superposition of $\tilde{I}(x)$ and $A(x)$, the Fourier transform of $a(k)$. At $x = \pm 2n\Delta x$, the shot noise is[5,6]

$$A(\pm 2n\Delta x) = ((\rho/e)S\Delta t R_R)^{1/2}\exp(-j\phi_{\text{rand}}). \quad (4)$$

ϕ_{rand} is the random phase of $A(\pm 2n\Delta x)$, and it is assumed that $R_R \gg R_S$. The phase error is at its maximum when $\phi_{\text{rand}} = 2k_0 n\delta x \pm \pi/2$ (i.e., $\tilde{I}$ and A are orthogonal), in which case the sensitivity of $\delta x(t)$ is

$$\delta x_{\text{sens}} = \frac{\lambda_0}{4n\pi}\arctan\left[\frac{|A(\pm 2n\Delta x)|}{|I_i(\pm 2n\Delta x)|}\right] \approx \frac{\lambda_0}{4n\pi}\left(\frac{2e}{\rho S\Delta t R_S}\right)^{1/2}, \quad (5a)$$

$$\delta x_{\text{sens}} \approx \frac{\lambda_0}{4n\pi}\left[\frac{1}{\text{SNR}(S, \Delta t, R_S)}\right]^{1/2}. \quad (5b)$$

The arctangent function arises in Eq. (5a) because phase noise can be visualized as the acute angle of a right triangle with the legs corresponding to the individual signal and noise vectors and the hypotenuse corresponding to the vector sum of signal and noise. Thus the displacement sensitivity of SDPM in the shot-noise limit is an explicit function of the signal-to-noise ratio (SNR) of the signal from the reflector whose displacement is being measured.

Both SS and FD setups were adapted to tabletop imaging optics on a floated table, while the FD setup was additionally adapted to a Zeiss Axiovert 200 microscope for the simultaneous acquisition of SDPM data and real-time video microscopy. We recorded $\delta x(t)$ by use of the following procedure: first, M samples of the spectral-domain signal were recorded. FD-OCT data were resampled to be evenly spaced in wave number. This signal was fast Fourier transformed to obtain the $M/2$-pixel complex-valued A-scan. After the reflection of interest in the A-scan (e.g., the cell–water interface) was identified, the A-scan pixel at the peak of this reflection was selected. This pixel represents the position of the interface to within the axial sampling resolution [i.e., $\pm n\Delta x$ in Eqs. (1)–(3)]. Lastly, the phase of this pixel was recorded as a function of time, and phase was converted to displacement by use of Eq. (3). The dis-

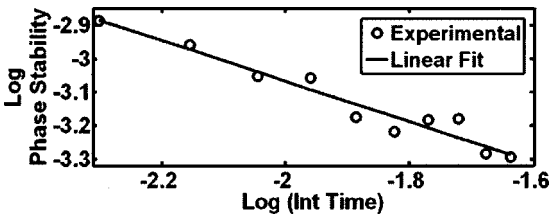

Fig. 2. Power relationship between the spectrometer integration time and measured phase stability of the SDPM signal generated by reflections from a coverslip.

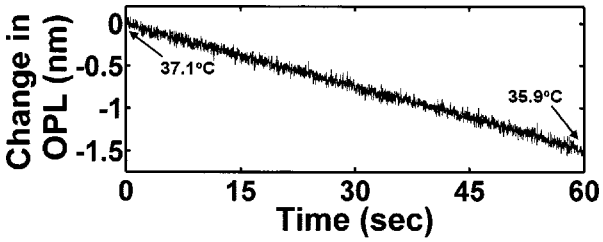

Fig. 3. Change in the OPL of a 213-μm borosilicate coverslip as the water bath is cooled 1.2°C.

placement stability was defined as the standard deviation of the displacement signal over time.

Figure 1 illustrates experimental measurements using a clean glass coverslip as a sample. With ~9 μW incident on the coverslip, the FD system had an observed displacement sensitivity of 53 pm, and with ~3 mW incident on the coverslip, the SS system had a displacement sensitivity of 780 pm. Despite these exquisite measured sensitivities, the experimental values remain significantly higher (by a factor of 6 and 7×10^4, respectively, for FD and SS configurations) than the shot-noise-limited performance predicted by Eq. (5a). Additional noise sources likely contributed to the experimentally detected signal, including $1/f$ noise in these homodyne systems, and any mechanical jitter in the sample-arm optics that was not mitigated by the common path topology. Further, the SS system performance was likely limited by scan-to-scan variability in the wavelength sweep, as any wavelength scan variability translates directly into reduced displacement sensitivity. This is an important design specification in SS laser design, given the increased interest in swept laser sources for spectral-domain OCT.

Equation (5a) indicates that the magnitude of the displacement stability noise floor is expected to be related to the square root of the reciprocal of the detector integration time. This is in contrast with the amplitude sensitivity, which is a linear function of detector integration time. We measured the displacement sensitivity of the FD system by use of a clean coverslip sample as a function of spectrometer integration time (Fig. 2). Equation (5a) predicts that the slope of $\log(\delta x_{\mathrm{sens}})$ versus $\log(\Delta t)$ should be -0.5. Even though this system was not operating in the shot-noise displacement sensitivity limit, the experimental line has a slope of -0.6, consistent with the theory prediction.

To demonstrate the displacement sensitivity of SDPM in a calibrated sample, we measured the thermal-expansion coefficient of a 213-μm-thick borosilicate coverslip using the microscope-adapted FD system. The coverslip served as the floor of a water bath on a heated microscope stage, and the change in the coverslip OPL was recorded as the water bath was cooled 1.2°C from 37.1 to 35.9°C (Fig. 3). The coverslip contracted 1.5 nm, yielding a thermal-expansion coefficient of $59\times10^{-7}/^{\circ}\mathrm{C}$, in good agreement with previously reported values.[7]

Measurement of cellular dynamics was performed on individual 2-day-old isolated chick embryo cardiomyocytes. A description of the isolation method was published previously.[8] Using SDPM, we measured submicrometer scale changes in cell thickness associated with spontaneous cardiomyocyte contraction at 37°C (Fig. 4). The cardiomyocyte depicted in Fig. 4 was spontaneously beating at ~0.3 Hz. The dynamics of contraction were well represented in the SDPM trace.

In conclusion, we have shown that spectral-domain OCT systems can be used to measure cellular motions with exquisite sensitivity. SDPM has several advantages over its time-domain counterparts. Its spectral domain approach has intrinsically higher phase stability than time-domain techniques. Additionally, the phase of spectral-domain common-path interferometry obviates the need for dual-beam interferometers that are necessary to achieve phase stability in time-domain approaches.

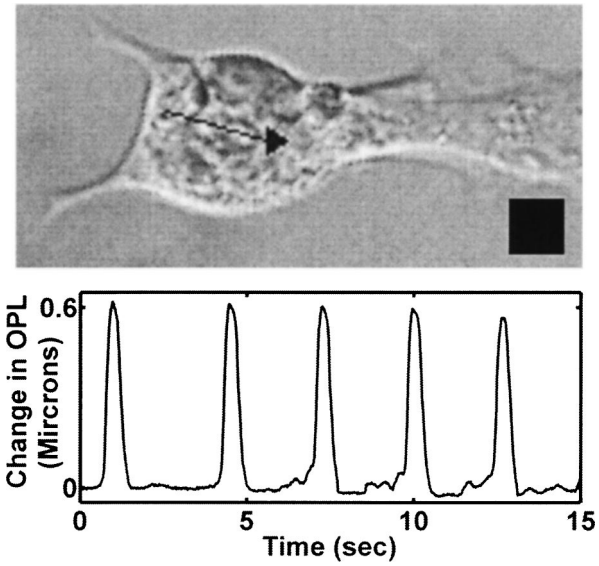

Fig. 4. Top, photomicrograph of an isolated cardiomyocyte from a chick embryo. The tip of the arrow denotes the location of the SDPM beam. The box is 10 μm $\times$ 10 μm. Bottom, change in thickness of beating cardiomyocyte measured with SDPM.

This work was supported by National Institutes of Health grants R24-EB000243 and R21-RR019769 to J. A. Izatt and grants R01 HL715015 and P01 HL36059 to T. L. Creazzo. M. A. Choma's e-mail address is mac32@duke.edu.

*Present address, Department of Electrical Engineering, California Institute of Technology, Pasadena, California 91125.

References

1. K. Svoboda, C. F. Schmidt, B. J. Schnapp, and S. M. Block, Nature **365**, 721 (1993).
2. J. Farinas and A. S. Verkman, Biophys. J. **71**, 3511 (1996).
3. C. Yang, A. Wax, M. S. Hahn, K. Badizadegan, R. R. Dasari, and M. S. Feld, Opt. Lett. **26**, 1271 (2001).
4. A. F. Fercher, C. K. Hitzenberger, G. Kamp, and S. Y. Elzaiat, Opt. Commun. **117**, 43 (1995).
5. M. A. Choma, M. V. Sarunic, C. Yang, and J. A. Izatt, Opt. Express **11**, 2183 (2003), http://www.opticsexpress.org.
6. R. Leitgeb, C. K. Hitzenberger, and A. F. Fercher, Opt. Express **11**, 889 (2003), http://www.opticsexpress.org.
7. O. V. Mazurin, M. V. Streltsina, and T. P. Shvaiko-Shvaikovskaya, *Handbook of Glass Data Part A* (Elsevier, New York, 1983).
8. T. L. Creazzo, J. Burch, and R. E. Godt, Biophys. J. **86**, 966 (2004).